

Reaction rate weighted multilayer nuclear reaction network

H. L. Liu,^{1,2} D. D. Han,^{3,*} Peng Ji,⁴ and Y. G. Ma^{1,†}

¹Key Laboratory of Nuclear Physics and Ion-beam Application (MOE),
Institute of Modern Physics, Fudan University, Shanghai 200433, China

²Shanghai Institute of Applied Physics, Chinese Academy of Sciences, Shanghai 201800, China

³School of Information Science and Technology, Fudan University, Shanghai 200433, China

⁴The Institute of Science and Technology for Brain-inspired Intelligence (ISTBI), Fudan University, Shanghai 200433, China

(Dated: October 13, 2020)

Nuclear reaction rate (λ) is a significant factor in the process of nucleosynthesis. A multi-layer directed-weighted nuclear reaction network in which the reaction rate as the weight, and neutron, proton, ^4He and the remainder nuclei as the criterion for different reaction-layers is for the first time built based on all thermonuclear reactions in the JINA REACLIB database. Our results show that with the increase of the stellar temperature (T_9), the distribution of nuclear reaction rates on the R -layer network demonstrates a transition from unimodal to bimodal distributions. Nuclei on the R -layer in the region of $\lambda = [1, 2.5 \times 10^1]$ have a more complicated out-going degree distribution than the one in the region of $\lambda = [10^{11}, 10^{13}]$, and the number of involved nuclei at $T_9 = 1$ is very different from the one at $T_9 = 3$. The redundant nuclei in the region of $\lambda = [1, 2.5 \times 10^1]$ at $T_9 = 3$ prefer (γ, p) and (γ, α) reactions to the ones at $T_9 = 1$, which produce nuclei around the β stable line. This work offers a novel way to the big-data analysis on nuclear reaction network at stellar temperatures.

The mechanism of the nucleosynthesis and nuclear astrophysics process has attracted a great interest. [1–15] Nuclear reaction rate, as an important input quantity in the calculation of the nuclear astrophysics network, can determine the path of nuclear reactions, and it can further affect the process of stellar evolution in the Universe and nuclear landscape. [16–19] Precise measurements of nuclear reaction rates as well as neutron-, proton- and photo-induced reaction cross sections have been intensively investigated in nuclear astrophysics [20–29] as well as superheavy element synthesis. [30–35] Additionally, features of α -clustering [36–40] and other exotic structures of light nuclei [41–46] as well as the determination of mass and binding energy [47–52] are related to nuclear astrophysics process. Several massive nuclear datasets, including REACLIB [53] and NACRE [54, 55] databases, have been constructed to facilitate this research topic. REACLIB database contains information about different reactions and the corresponding reaction rate parameters, maintained by the Joint Institute for Nuclear Astrophysics (JINA). In this work, we use the data from REACLIB V2.0, which includes 8048 nuclei and 82851 nuclear reactions, in which the detailed information related to reaction rate consisting of reaction types, reactants and products, and Q -value are provided. [53]

On the other hand, complex network science has achieved significant advances in recent years. [56–59] Various real systems, such as internet, social connections, epidemics spreading, and chemical reactions etc. can be treated as complex networks to facilitate investigations. [60–66] The main idea of the complex network construction is to consider units as nodes and the interaction between two units as an edge. Furthermore, many features of real systems can be investigated by taking advantage of the topological characteristics of the

network, and this can further uncover some hidden properties. In our previous work, using the REACLIB, we considered four layers (N -layer, P -layer, H -layer and R -layer), and then formulated a multi-layer directed non-weighted nuclear reaction networks via the substrate-product method, moreover, solely studied its topological features. [67] The reaction rate, however, is an important input quantity in the process of nucleosynthesis, which remains to be taken into account during the construction of the nuclear reaction network.

Previous nuclear astrophysics studies mainly concentrated on the precise calculation of nuclear reaction rates involve different types of nuclear reactions. [54, 68] In this Letter, however, we focus on the topological characteristics of the directed-weighted nuclear reaction network with the reaction rate as the weight and particularly conduct statistical analysis of the reaction path of the nuclei.

The reactions in the REACLIB database, in general, are reversible and contain forward and backward directions. For the forward reaction, the reaction rate λ can be calculated by a parametrized function, which contains seven parameters a_0 - a_6 shown as follows [69]:

$$\lambda = \exp(a_0 + \sum_{i=1}^5 a_i T_9^{\frac{2i-5}{3}} + a_6 \ln T_9) \quad (1)$$

where $a_0 \sim a_6$ are given in the REACLIB database and the T_9 given in a unit of 10^9K represents stellar temperature where nuclei take part in different reactions. Although, these parameters for the backward reaction are not presented directly in the REACLIB database, the reverse reaction rate can be computed with the help of the partition functions in the file of WINVN. [69, 70] The value of reverse reaction rate is equal to the forward reaction rate times the partition functions.

In general, the fitted reaction rates are only valid in region of some temperatures, and REACLIB database provides 24 temperatures T_9 including 0.1, 0.15, 0.2, 0.3, 0.4, 0.5, 0.6, 0.7, 0.8, 0.9, 1.0, 1.5, 2.0, 2.5, 3.0, 3.5, 4.0, 4.5, 5.0, 6.0, 7.0, 8.0, 9.0, and 10.0. In the present manuscript, we only discuss the results at $T_9 = 0.1, 1$ and 3.

In our previous directed non-weighted nuclear reaction network based on REACLIB and the substrate-product method, all nuclear reactions were divided to four types of N -layer, P -layer, H -layer and R -layer, which denote, respectively, the reactant of the neutron, proton, ^4He and reminders. For each nucleus (or ‘node’ X in terms of network concept), we can identify whether the N -layer reaction is the ‘in-coming’ (e.g $n + Y \rightarrow X$), or ‘out-going’ ($X + n \rightarrow Y$). The number of reactions for each nucleus (node) is represented by the number of ‘degree’ which is divided into either in-coming degree or out-going degree. With this definition, the in-coming and out-going degree distributions of nuclei in the nuclear landscape can be accumulated for each layer of nuclear reaction network. In this Letter, we establish a directed-weighted nuclear reaction network where nuclear reaction rate is taken as the weight of edges, which is based on the following consideration: the existence of edges of the nuclear reaction network indicates that a certain reaction can take place, and the magnitude of nuclear reaction rate quantifies the reaction probability of this reaction, and the corresponding edge is more important in the weighted network.

Considering that the R -layer network has more complicated structure in comparison with the N -layer, P -layer and H -layer in a directed non-weighted nuclear reaction network [67, 71–73], here we also focus the R -layer topology in the framework of directed-weighted network. In what follows, we perform the analysis on R -layer network in which the nuclei mainly involve in photodisintegration reactions and β decay reactions process under different temperature T_9 .

On the basis of the reaction rate equation (1), each nuclear reaction rate in the R -layer network can be obtained at different temperatures combining with the REACLIB and WINVN databases. We found that the reaction rate has a heterogeneous distribution, ranging from 10^{-100} to 10^{50} . For an example, Fig. 1 demonstrates such distribution of nuclei in the R -layer network at three values of $T_9 = 0.1, 1.0$ and 3.0. From the perspective of stellar element burning process, the above temperatures are close to the threshold of He- ($0.15 \sim 0.23 T_9$) [74], Ne- ($1.4 \sim 1.7 T_9$) [75] and Si- ($\sim 3.0 T_9$) [76] burning processes. Figure 1 indicates that the distribution of reaction rates of all nuclei varying from a unimodal distribution to a bimodal distribution with the increases of T_9 from 0.1 to 3.0. This results in many questions: does the second peak at high temperatures come from the same nuclei as for the first peak but due to the increasing of nuclear reaction rate, or come from other nuclei not for the first peak? Whether are the nuclei in the regions of the two peaks

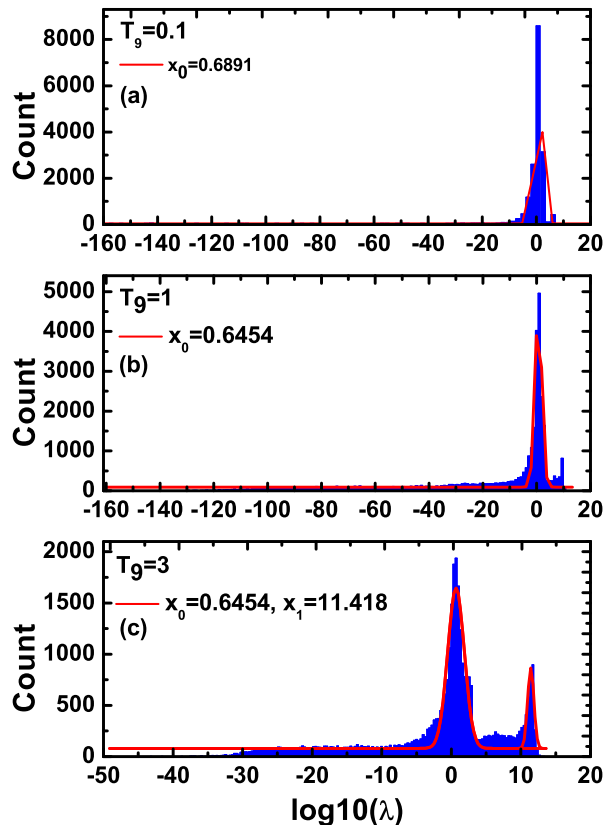


FIG. 1. Distribution of reaction rates of all nuclei with the Gaussian fits in the R -layer at three different T_9 : 0.1 (a), 1.0 (b), and 3.0 (c). From the fits, it indicates the positions of the peaks for $T_9 = 0.1$ and 1.0 are $\lambda = 10^{0.6891}$ and $10^{0.6454}$, respectively, while positions of the double peaks for $T_9 = 3$ are $\lambda = 10^{0.6714}$ and $10^{11.418}$.

same or the same type of reactions? What is the degree distribution of the nuclei in the region of two peaks at different temperatures? In order to address these questions, we perform Gaussian fits to the peak distributions shown in Fig. 1.

It shows that the central values of the peaks are $\lambda = 10^{0.6454}$ for $T_9 = 1$, $\lambda = 10^{0.6714}$ and $10^{11.418}$ for $T_9 = 3$, respectively. For the first peak at three temperatures, the positions of peak vary not much, however, for the second peak which emerges at $T_9 = 3$, the position of peak is much larger. In the directed-weighted R -layer network, the direction is from reactant to product and the weight represents the capability of reactant to product. Therefore, the reaction-rate distribution illustrates the attribute of the reactants, and the difference of reaction rate might express the different reactions of nuclei which can be indicated by the difference of the out-going degrees of nuclei in the network. There is a hypothesis that the reactions with $\lambda \leq 10^{-18}$ is unable to occur because these reactions will not change anything within time scale of astrophysical process. In this work, we focus on the regions of $\lambda = [10^0, 2.5 \times 10^1]$ for $T_9 = 1$, $\lambda = [10^0, 2.5 \times 10^1]$

and $\lambda = [10^{11}, 10^{13}]$ for $T_9 = 3$, respectively, to study the nuclei's distribution with the number of nuclei more than 80 percents of total mounts. Taking the advantage of the directed-weighted R -layer network, we compute the nuclei's out-going degree in the selected reaction rate's region, as shown in the nuclei's chart. Figure 2 demonstrates the out-going degree distributions of the nuclei in the regions of $\lambda = [10^0, 2.5 \times 10^1]$ for $T_9 = 1$ as well as $\lambda = [10^0, 2.5 \times 10^1]$ and $\lambda = [10^{11}, 10^{13}]$ for $T_9 = 3$. The nuclei in the first region of $\lambda = [10^0, 2.5 \times 10^1]$ display rich out-going degrees which have a maximum being equal to 5. However, all nuclei in the second region show the same out-going degrees being equal to 1. Such phenomenon reflects that the nuclei in the region of $\lambda = [10^0, 2.5 \times 10^1]$ at $T_9 = 1$ and $T_9 = 3$ can participate in multiple reactions, but the nuclei in the region of $\lambda = [10^{11}, 10^{13}]$ at $T_9 = 3$ just take part in one kind of reaction. The nuclei around the β stable line emerge in the first peak region at $T_9 = 3$ but it does not appear at $T_9=1$. By comparing the nuclei in the regions of two peaks on the nuclear landscape at $T_9 = 3$, we find that there are differences in nuclei's distribution which implies that they may participate in different reactions.

Furthermore, in order to demonstrate the influences of temperature and reaction rates, we perform the degree differences between Fig. 2(b) and (a), and plot them in upper panels of Fig. 3. Figure 3(a) shows the part of positive degree difference and (b) shows the part of negative degree difference. Figure 3(a) indicates that the nuclei around the β stable line emerge from $T_9 = 1$ to $T_9 = 3$ and stable nuclei more vulnerable to decay at high temperatures. Meanwhile, the elements in the neutron-rich region vanish and some proton-rich nuclei decline as shown in Fig. 3(b). In the same way, the degree differences between Fig. 2(c) and (b) are divided into two panels: Fig. 3(c) shows the part of positive degree difference and Fig. 3(d) shows the part of negative degree difference. From those two panels, small portions of proton-rich and neutron-rich nuclei are produced as plotted by all markers in Fig. 3(c) at higher nuclear reaction rates, i.e $\lambda = [10^{11}, 10^{13}]$, but the nuclei around the β stable line, and dominant neutron-rich nuclei as well as some proton-rich nuclei disappear as plotted by all markers in Fig. 3(d). These phenomena evidenced that neutron-rich and proton-rich nuclei can occur reactions with high reaction rates.

All reaction types in astrophysical investigations are (n, γ) , (n, p) , (n, α) , (p, γ) , (p, n) , (p, α) , (α, γ) , (α, n) , (α, p) , (γ, n) , (γ, p) , (γ, α) , β^+ and β^- . The main reaction types in the R -layer network, by using of the reactant-product method, include the reactions (γ, n) , (γ, p) , (γ, α) , β^+ and β^- . Previously, we systematically introduced the nuclei's distribution on the nuclei chart which can react at different temperatures or reaction rates. In order to explain concretely the reaction type which nuclei are involved, we specify the types of reactions that

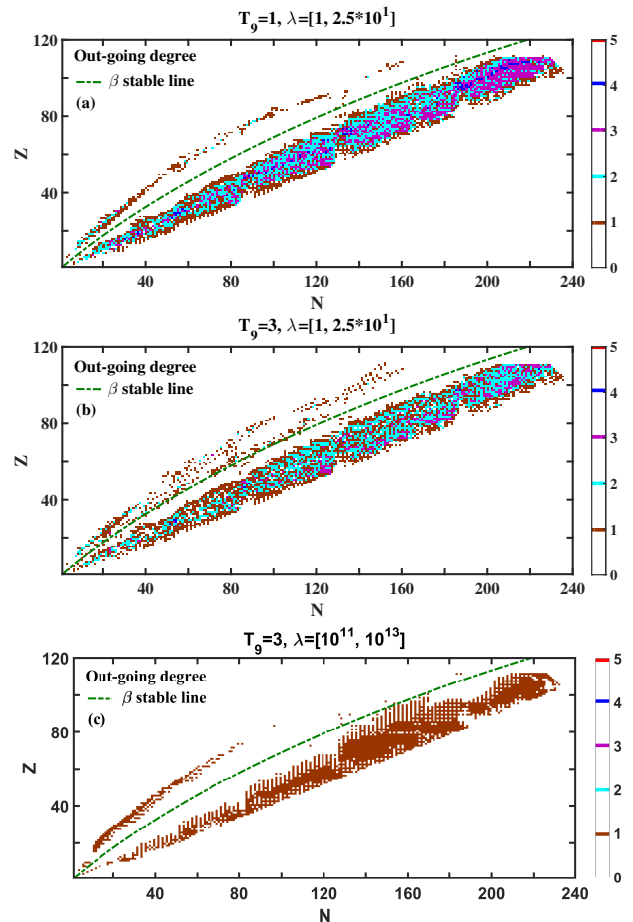


FIG. 2. Out-going degree distributions of R -layer on a N - Z plane in different windows of reaction rate (λ) and temperature (T_9). (a) $\lambda = [10^0, 2.5 \times 10^1]$ and $T_9 = 1$; (b) $\lambda = [10^0, 2.5 \times 10^1]$ and $T_9 = 3$; (c): $\lambda = [10^{11}, 10^{13}]$ and $T_9 = 3$. The out-going degrees are calculated for each nucleus and the values are indicated by color and calibrated in the right border of the figure. x - and y -axis represent the number of neutrons (N) and protons (Z) of that nucleus. The β stable line is also plotted in figure.

each nucleus can participate in. Table I shows the detailed information of each reaction type in the R -layer, where δA and δZ are the difference in mass and proton numbers of the reactants and products, respectively.

TABLE I. The classification of reaction types depending on the difference of mass number and proton number between reactant and production.

Reaction type	δA	δZ
(γ, n)	1	0
(γ, p)	1	1
(γ, α)	4	2
β^+	0	1
β^-	0	-1

According to the classical method of nuclear reaction types in Tab. I, we conduct a statistical analysis of the

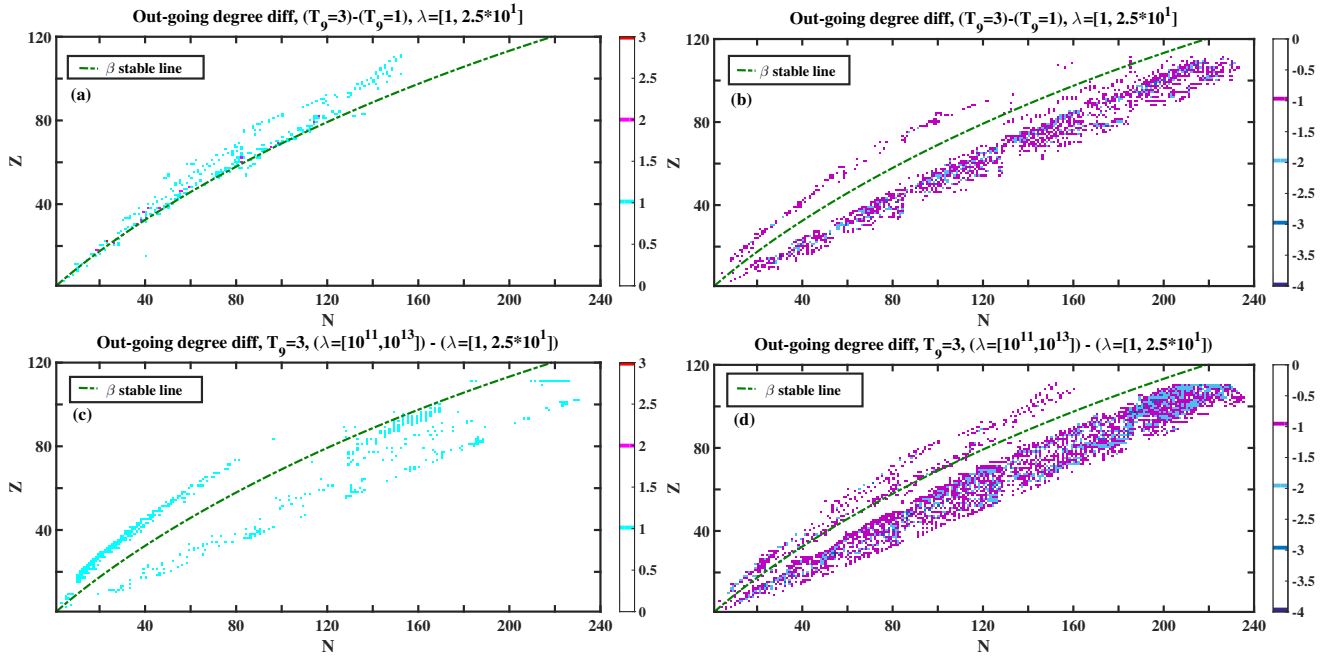


FIG. 3. Difference of out-going degrees between different regions of λ and T_9 . (a) positive degree difference between $T_9 = 3$ and $T_9 = 1$ in the region of $\lambda = [10^0, 2.5 \times 10^1]$; (b) same as (a) but for the part of negative degree difference; (c) positive degree difference between the regions of $\lambda = [10^{11}, 10^{13}]$ and $[10^0, 2.5 \times 10^1]$ at $T_9 = 3$; (d) same as (c) but for the part of negative degree difference.

reactions which each nucleus can take part in at different temperatures. The nuclei's distribution of all reaction types in the nuclear chart is shown in Fig. 4. Different colors represent different nuclear reactions, and more detailed information can be found in Fig. 4. In Fig. 4(a) and (b), most of the nuclei in the reaction rate region of $[10^0, 2.5 \times 10^1]$ can participate in multiple reactions (i.e. some nuclei can participate in other reactions which not shown in Tab. I). For instance, these nuclei may decay multiple neutrons, protons or heliums. By comparing Fig. 4(a) with (b), we found that the accessorial nuclei mainly take part in reactions of (γ, p) and (γ, α) , and these reactions are responsible for the emergence of the nuclei around the β stable line at $T_9 = 3$. On the other hand, it illustrates that the nuclei which take part in (γ, n) reaction at $T_9 = 1$ have a significantly difference with respect to that at $T_9 = 3$.

For the nuclei's distribution at the same temperature $T_9 = 3$, the nuclei within two regions of nuclear reaction rates have different (N, Z) distributions shown in Fig. 4(b) and (c). The nuclei in neutron-rich region are more likely to have (γ, n) reaction at higher temperature which can be attributed by the high neutron-proton ratio. Moreover, combining the nuclei's distributions of Fig. 4(a) with those of Fig. 4(b) and (c), we can see that the (γ, n) reaction for proton-rich nuclei can occur at higher temperature the same as the neutron-rich nuclei. The nuclei, on the whole, in the first peak mainly involve β decay, which are largely temperature independent in

the JINA database. And the nuclei in the second peak are due to photodisintegration reactions, which become important at higher temperatures. Specific numbers of the nuclei of each reaction type are shown in Tab. II, which displays that the nuclei in the reaction rate region of $[10^{11}, 10^{13}]$ only take part in one reaction. According to the nuclei region and temperatures, the nuclear processes for neutron-rich and proton-rich nuclei are corresponding to r-process and rp-process. Both processes are the competition between β decay and nucleon capture reactions.

TABLE II. The reaction types at $T_9 = 1$ and 3 with different λ in the R-layer network.

Reaction type	$T_9 = 1$ $\lambda = [10^0, 25]$	$T_9 = 3$ $\lambda = [10^0, 25]$	$T_9 = 3$ $\lambda = [10^{11}, 10^{13}]$
(γ, n)	243	144	2324
(γ, p)	35	77	221
(γ, α)	83	162	1
β^+	162	111	
β^-	2487	2232	
all	7331	5781	2546

In summary, we constructed a new nuclear reaction-rate weighted multi-layer network based on the substrate-product method, which consists of all nuclei and reactions in the JINA REACLIB database. The nuclear reaction networks are set up with four layers of N -layer, P -layer, H -layer and R -layer, depending on the reactants of the neutron, proton, ${}^4\text{He}$ or the reminder nuclei,

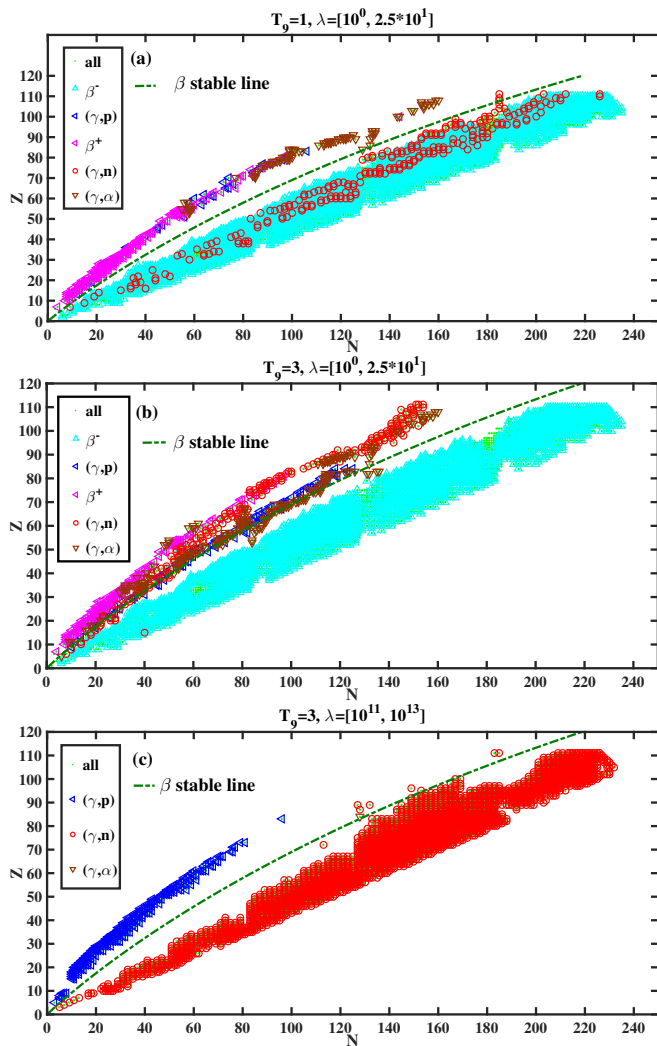


FIG. 4. Nuclei's distributions of the R -layer on a N - Z plane in different windows of reaction rate (λ) and temperature (T_9). (a): $\lambda = [10^0, 2.5 \times 10^1]$ and $T_9 = 1$. (b): $\lambda = [10^0, 2.5 \times 10^1]$ and $T_9 = 3$, and (c): $\lambda = [10^{11}, 10^{13}]$ and $T_9 = 3$. The different reaction types are indicated by different markers with colors.

respectively. Our special focus is on the R -layer reaction network since it has rich topological features. It is found that the weights of the nuclear reaction network display a heterogeneous distribution. Interestingly, with the increase of the T_9 , the reaction rates of the R -layer network exhibit a transition from unimodal distribution around $\lambda = [10^0, 2.5 \times 10^1]$ to bimodal distribution with one peak around $\lambda = [10^0, 2.5 \times 10^1]$ and another around $\lambda = [10^{11}, 10^{13}]$. Based on the analysis of the nuclei within the bimodal peaks of nuclear reaction rates, we found that the nuclei within the first peak at $T_9 = 1$ and $T_9 = 3$ have a complicated out-going degree in comparison with the nuclei in second peak at $T_9 = 3$, in which the out-going degree is equal to one. By classifying all reactions in the R -layer at the same temperature $T_9 = 3$,

we found that the nuclei in the region of two nuclear reaction rates locate at very different (N, Z) positions. By comparing out-going degree distribution of nuclei at different temperatures of $T_9 = 1$ and 3, it is found that the nuclei mainly take part in reactions of (γ, p) and (γ, α) at $T_9 = 3$ which are responsible for the emergence of the nuclei around the β -stable line. With the nuclear reaction rates approaching $\lambda = [10^{11}, 10^{13}]$, the nuclei around the β stable line as well as the β decays fade away, and the nuclei in neutron-rich region are mostly have only (γ, n) reaction, which becomes the main reason of the instability of neutron-rich nuclei.

We emphasize that the current work is not for making a specific diagnosis nucleus by nucleus, but for demonstrating a kind of big-data statistical analysis of the nuclear chart. In addition, caution should be taken because of the lack of some exotic nuclear reaction data and the extrapolation uncertainty of reaction rates in the current database-driven analysis. It is expected that more and more unstable nuclear reaction and decay data will be accumulated with the application of radioactive ion beam accelerator, which will certainly further improve the network analysis. Overall, the present work sheds light on that a novel way for the topological structure analysis of nuclear reaction network at different stellar temperatures by a marriage of a known nuclear reaction-rate database to the knowledge of complex network science.

Acknowledgments: This work is supported by the National Natural Science Foundation of China under Contracts Nos. 11890714, 11421505, 11875133 and 11075057, the National Key R&D Program of China under Grant No. 2018YFB2101302, the Key Research Program of Frontier Sciences of the CAS under Grant No. QYZDJ-SSW-SLH002, and the Strategic Priority Research Program of the CAS under Grant No XDB34030200.

* ddhan@fudan.edu.cn

† mayugang@fudan.edu.cn

- [1] Burbidge E M, Burbidge G R, Fowler W A and Hoyle F 1957 *Rev. Mod. Phys.* **29** 547
- [2] Schatz H, Aprahamian A, Görres J, *et al.*, 1998 *Phys. Rep.* **294** 167
- [3] Arnould M, Goriely S and Takahashi K 2007 *Phys. Rep.* **450** 97
- [4] Käppeler F, Gallino R, Bisterzo S and Aoki W 2011 *Rev. Mod. Phys.* **83** 157
- [5] Chen J, Keane D, Ma Y G, Tang A and Xu Z 2018 *Phys. Rep.* **760** 1
- [6] Ji A P, Frebel A, Chiti A and Simon J D 2016 *Nature* **531** 610
- [7] Pian E, Avanzo P D, Benetti S, *et al.* 2017 *Nature* **551** 67 (2017).
- [8] Fynbo H, Diget C A, Bergmann U C, Borge M J G, *et al.* (ISOLDE Collaboration) 2005 *Nature* **433** 136
- [9] An Z D, Chen Z P, Ma Y G, Yu J K, *et al.* 2015 *Phys.*

- Rev. C* **92** 045802
- [10] Pais H, Gulminelli F, Providencia C and Röpke G 2018 *Nucl. Sci. Tech.* **29** 181
- [11] Tang X D, Ma S B, Fang X, Bucher B, Alongi A, Cahillane C and Tan W -P 2019 *Nucl. Sci. Tech.* **30** 126
- [12] Ma S B, Zhang L Y and Hu J 2019 *Nucl. Sci. Tech.* **30** 141
- [13] Li W J, Ma Y G, Zhang G Q, Deng X G, *et al.* 2019 *Nucl. Sci. Tech.* **30** 180
- [14] Ding W B, Yu Z, Xu Y, Liu C J and Bao T 2019 *Chin. Phys. Lett.* **36** 049701
- [15] Jiang Y, Lou J L, Ye Y L, Pang D Y, *et al.* 2018 *Chin. Phys. Lett.* **35** 082501
- [16] Hotokezaka K, Piran T and Paul M 2015 *Nat. Phys.* **11** 1042
- [17] Kienle P, Faestermann T, Friese J, Korner H J, *et al.* 2001 *Prog. Part. Nucl. Phys.* **46** 73
- [18] Erler J, Birge N, Kortelainen M, Nazarewicz W, Olsen E, Perhac A M and Stoitsov M 2012 *Nature* **486** 509
- [19] Wang R and Chen L W 2015 *Phys. Rev. C* **92** 031303(R)
- [20] Spergel D N, Verde L, Peiris H V, Komatsu E, Nolte M R, *et al.* 2003 *Astrophys. J. Suppl.* **148** 175
- [21] SDSS Collaboration, website: <http://www.sdss.org/>.
- [22] Serpico P D, Esposito S, Iocco F, Mangano G, Miele G and Pisanti O 2004 *Journal of Cosmology and Astroparticle Physics*, **12** 010.
- [23] Guo H R, Han Y L and Cai C H 2019 *Nucl. Sci. Tech.* **30** 13
- [24] Baldik R and Yilmaz A 2018 *Nucl. Sci. Tech.* **29** 156
- [25] Yalcin C 2017 *Nucl. Sci. Tech.* **28** 113
- [26] Best A, Pantaleo F R, Boeltzig A, Imbriani G, Aliotta M, *et al.* 2019 *Phys. Lett. B* **797** 134900
- [27] Marcucci L E, Mangano G, Kievsky A and Viviani M 2016 *Phys. Rev. Lett.* **116** 102501
- [28] Bennett M B, Wrede C and Brown B A 2016 *Phys. Rev. Lett.* **116** 102502
- [29] Huang B S, Ma Y G and He W B 2017 *Phys. Rev. C* **95** 034606
- [30] Giuliani S A, Matheson Z, Nazarewicz W, *et al.* 2019 *Rev. Mod. Phys.* **91** 011001
- [31] Oganessian Yu Ts, Abdullin F Sh, Bailey P D, Bennett M E, *et al.* 2010 *Phys. Rev. Lett.* **104** 142502
- [32] Yu X B, Zhu L, Wu Z H, Li F, Su J and Guo C C 2018 *Nucl. Sci. Tech.* **29** 154
- [33] Naderi D and Alavi S A 2018 *Nucl. Sci. Tech.* **29** 161
- [34] Boilley D, Cauchois B, Lü H, Marchix A, Abe Y and Shen C 2018 *Nucl. Sci. Tech.* **29** 172
- [35] Kasen D, Metzger B, Barnes J, Quataert E and Ramirez-Ruiz E 2017 *Nature* **551** 80
- [36] Elhatisari S, Lee D, Rupak G, Epelbaum E, Krebs H, Lähde T A, Luu T and Meißner Ulf-G, 2015 *Nature* **528** 111
- [37] Epelbaum E, Krebs H, Lee D and Meißner Ulf-G 2011 *Phys. Rev. Lett.* **106** 192501
- [38] He W B, Ma Y G, Cao X G, Cai X Z and Zhang G Q 2014 *Phys. Rev. Lett.* **113** 032506
- [39] Liu Y and Ye Y L 2018 *Nucl. Sci. Tech.* **29** 184
- [40] Zhang S, Wang J C, Bonasera A, Huang M R, *et al.* 2019 *Chin. Phys. C* **43** 064102
- [41] Ma Y G, Fang D Q, Sun X Y, Zhou P, *et al.* 2015 *Phys. Lett. B* **743** 306
- [42] Li Z H, Li Y J, Su J, Yan S Q, Wang Y B, Guo B, Nan D, *et al.* 2019 *Sci. China Phys. Mech. Astron.* **62** 32021
- [43] Jiang W, Ye Y, Li Z H, Lin C J, *et al.* 2017 *Sci. China Phys. Mech. Astron.* **60** 062011
- [44] Yun X, Pang D Y, Xu Y P, Zhang Z, Xu R R, Ma Z Y and Yuan C X 2020 *Sci. China Phys. Mech. Astron.* **63** 222011
- [45] Wei L, Lou J L, Ye Y L and Pang D Y 2020 *Nucl. Sci. Tech.* **31** 20
- [46] Wang Y T, Fang D Q, Xu X X, Sun L J, Wang K, *et al.* 2018 *Nucl. Sci. Tech.* **29** 98
- [47] Wu D, Bai C L, Sagawa H, Song Z Q and Zhang H Q 2020 *Nucl. Sci. Tech.* **31** 14
- [48] Benzaid D, Bentriddi S, Kerraci A and Amrani N 2020 *Nucl. Sci. Tech.* **31** 9
- [49] Liu P, Chen J, Keane D, Xu Z and Ma Y G 2019 *Chin. Phys. C* **43** 124001
- [50] Martin D, Arcones A, Nazarewicz W and Olsen E 2016 *Phys. Rev. Lett.* **116** 121101
- [51] Block M, Ackermann D, Blaum K, Droese C, Dworschak M, *et al.* 2010 *Nature* **463** 784
- [52] Tu X L, Xu H S, Wang M, Zhang Y H, *et al.* 2011 *Phys. Rev. Lett.* **106** 112501
- [53] Cyburt R H, Amthor A M, Ferguson R, Meisel Z, Smith K, *et al.* 2010 *The Astrophysical Journal Supplement Series* **189** 240
- [54] Angulo C, Arnould M, Rayet M, Descouvemont P, *et al.* 1999 *Nucl. Phys. A* **656** 3
- [55] Xu Y, Takahashi K, Goriely S, Arnould M, Ohta M and Utsunomiya H 2013 *Nucl. Phys. A* **918** 61
- [56] Barabási A L and Albert R 1999 *Science* **286** 509
- [57] Boccaletti S, Latora V, Moreno Y, Chavez M and Hwang D U 2006 *Phys. Rep.* **424** 175
- [58] Costa L D, Oliveira O N, Travieso G, Rodrigues F A, *et al.* 2011 *Adv. Phys.* **60** 329
- [59] Barabási A L 2016 *Network Science* (Cambridge University Press)
- [60] Watts D J and Strogatz S H 1998 *Nature* **393** 440
- [61] Jolley C C and Douglas T 2010 *APJ* **722** 1921
- [62] Jolley C and Douglas T 2012 *Astrobiology* **12** 29
- [63] Han D D, Liu J G, Ma Y G, Cai X Z and Shen W Q 2004 *Chin. Phys. Lett.* **21** 1855
- [64] Han D D, Liu J G and Ma Y G 2008 *Chin. Phys. Lett.* **25** 76
- [65] Qian J H, Han D D and Ma Y G 2012 *Europhys. Lett.* **100** 48006
- [66] Qian J H, Chen Q, Han D D, Ma Y G and Shen W Q 2014 *Phys. Rev. E* **89** 062808
- [67] Zhu L, Ma Y G, Chen Q and Han D D 2016 *Sci. Rep.* **6** 31882
- [68] Guo B, Li Z H, Bai X X, Liu W P, Shu, N C and Chen Y S 2006 *Phys. Rev. C* **73** 048801
- [69] Thomas R and Thielemann F K 2000 *Atomic Data and Nuclear Data Tables* **75** 1
- [70] Rauscher T and Thielemann F K 2001 *Atomic Data and Nuclear Data Tables* **79** 47
- [71] Liu H L, Han D D, Ma Y G and Zhu L 2020 *Sci. China Phys. Mech. Astron.* **63** 112062
- [72] Bertulani C A 2020 *Sci. China Phys. Mech. Astron.* **63** 112063
- [73] Long G L 2020 *Sci. China Phys. Mech. Astron.* **63** 112061
- [74] Austin S M, West C and Heger A 2014 *Phys. Rev. Lett.* **112** 111101
- [75] F. Ferraro, M. P. Takács, D. Piatti, Cavanna F, Aliotta M, *et al.* 2018 *Phys. Rev. Lett.* **121** 172701
- [76] Bodansky D, Clayton D D and Fowler W A 1968 *Phys. Rev. Lett.* **20** 161